Bioorganic & Medicinal Chemistry 19 (2011) 5125–5136

Contents lists available at ScienceDirect

Bioorganic & Medicinal Chemistry

journal homepage: www.elsevier.com/locate/bmc

Halogen-substituted (*C*-β-D-glucopyranosyl)-hydroquinone regioisomers: Synthesis, enzymatic evaluation and their binding to glycogen phosphorylase

Kyra-Melinda Alexacou [a,b], Yun Zhi Zhang [c,d,e,f], Jean-Pierre Praly [c,d,e,f,*], Spyros E. Zographos [a], Evangelia D. Chrysina [a], Nikos G. Oikonomakos [a,✠], Demetres D. Leonidas [g,*]

[a] *Institute of Organic and Pharmaceutical Chemistry, National Hellenic Research Foundation, 48 Vassileos Constantinou Avenue, 11635 Athens, Greece*
[b] *Department of Biology, Chemistry and Pharmacy, Freie Universität Berlin, Takustr. 3, 14195 Berlin, Germany*
[c] *Université de Lyon, Institut de Chimie et Biochimie Moléculaires et Supramoléculaires associé au CNRS, UMR 5246, Laboratoire de Chimie Organique 2-Glycochimie, Bâtiment Curien, 43 boulevard du 11 Novembre 1918, F-69622 Villeurbanne, France*
[d] *Université Lyon 1, F-69622 Villeurbanne, France*
[e] *CNRS, UMR5246, Institut de Chimie et Biochimie Moléculaires et Supramoléculaires (ICBMS), Laboratoire de Chimie Organique 2-Glycochimie, Bâtiment Curien, 43 boulevard du 11 Novembre 1918, F-69622 Villeurbanne, France*
[f] *CPE-Lyon, F-69616 Villeurbanne, France*
[g] *Department of Biochemistry and Biotechnology, University of Thessaly, 26 Ploutonos Str. 41221 Larissa, Greece*

ARTICLE INFO

Article history:
Received 18 May 2011
Revised 12 July 2011
Accepted 13 July 2011
Available online 21 July 2011

Keywords:
Type 2 diabetes
Glycogen phosphorylase
C-glucosyl aryl
C-glucopyranosyl hydroquinone
Inhibition
X-ray crystallography

ABSTRACT

Electrophilic halogenation of *C*-(2,3,4,6-tetra-*O*-acetyl-β-D-glucopyranosyl) 1,4-dimethoxybenzene (**1**) afforded regioselectively products halogenated at the *para* position to the D-glucosyl moiety (**8**, **9**) that were deacetylated to **3** (chloride) and **16** (bromide). For preparing *meta* regioisomers, **1** was efficiently oxidized with CAN to afford *C*-(2,3,4,6-tetra-*O*-acetyl-β-D-glucopyranosyl) 1,4-benzoquinone **2** which, in either MeOH or H_2O–THF containing few equivalents of AcCl, added hydrochloric acid to produce predominantly *meta* (with respect to the sugar moiety) chlorinated hydroquinone derivatives **5** and **18**, this latter being deacetylated to **4**. The deacetylated *meta* (**4**, **5**) or *para* (**3**, **16**) halohydroquinones were evaluated as inhibitors of glycogen phosphorylase (GP, a molecular target for inhibition of hepatic glycogenolysis under high glucose concentrations) by kinetics and X-ray crystallography. These compounds are competitive inhibitors of GPb with respect to α-D-glucose-1-phosphate. The measured IC_{50} values (μM) [169.9 ± 10.0 (**3**), 95 (**4**), 39.8 ± 0.3 (**5**) 136.4 ± 4.9 (**16**)] showed that the *meta* halogenated inhibitors (**4**, **5**) are more potent than their *para* analogs (**3**, **16**). The crystal structures of GPb in complex with these compounds at high resolution (1.97–2.05 Å) revealed that the inhibitors are accommodated at the catalytic site and stabilize the T conformation of the enzyme. The differences in their inhibitory potency can be interpreted in terms of variations in the interactions with protein residues of the different substituents on the aromatic part of the inhibitors.

1. Introduction

The most common type of diabetes is type 2 diabetes mellitus (T2DM) and it accounts for approximately 90–95% of diabetes cases.[1,2] It is characterized by abnormal insulin secretion and/or insulin resistance. The combination of pancreatic β-cell dysfunction and insulin resistance by namely skeletal muscle, the liver and fat tissue, gives rise to increased blood glucose. The number of diabetic cases has been increasing exponentially over the past years and it is estimated that by the year 2030 the number of prevalent patients will reach 300 million.[3] The commonly prescribed hypoglycemic agents (biguanides, sulfonylureas, thiazolidinediones, α-glucosidase inhibitors) for symptomatic treatment of diabetes[4,5] have undesirable side effects and are inadequate for 30–40% of patients.[6] This inadequacy of the current pharmacological agents for the treatment of T2DM is an incentive for research efforts towards new therapies.

Glycogen phosphorylase (GP) is a regulatory enzyme that catalyzes the first step of the intracellular degradation of glycogen, an important source of glucose production. This enzyme is found in

Abbreviations: GP, glycogen phosphorylase; GPb, rabbit muscle glycogen phosphorylase b; PLP, pyridoxal 5′-phosphate; Glc-1-P, α-D-glucose 1-phosphate; rmsd, root–mean–square deviation.

* Corresponding authors. Address: Department of Biochemistry and Biotechnology, University of Thessaly, 26 Ploutonos Str., 41221 Larissa, Greece. Tel.: +30 2410 565278; fax: +30 2410 565290 (D.D.L.); Université de Lyon, Institut de Chimie et Biochimie Moléculaires et Supramoléculaires associé au CNRS, UMR 5246, Laboratoire de Chimie Organique 2-Glycochimie, Bâtiment Curien, 43 boulevard du 11 Novembre 1918, F-69622 Villeurbanne, France. Tel.: +33 (0) 4 72 43 11 61; fax : +33 (0) 4 72 43 27 52 (J.-P.P.).

E-mail addresses: jean-pierre.praly@univ-lyon1.fr (J.-P. Praly), ddleonidas@bio.uth.gr (D.D. Leonidas).

✠ Deceased on August 31st 2008

0968-0896/$ - see front matter © 2011 Elsevier Ltd. All rights reserved.
doi:10.1016/j.bmc.2011.07.024

every species from unicellular organisms and bacteria to the complex tissues of higher plants and mammals, where it plays a key role in carbohydrate metabolism. The best studied example of glycogen phosphorylase is the rabbit muscle enzyme, which was first isolated and characterized by G.T. Cori and C.F. Cori in 1936.[7] Rabbit muscle GP is a dimer composed of two identical subunits 842 amino acids each, and a co-factor, pyridoxal 5′-phosphate (PLP). It is regulated allosterically by phosphorylation and it exists in two forms: the unphosphorylated T state GPb and the phosphorylated R state GPa.[8] A large number of compounds have been reported to bind at five distinct binding sites: the catalytic, the allosteric, and the new allosteric, the inhibitor and the glycogen storage site.[9,10] The efficacy of such inhibitors on blood glucose control and hepatic glycogen balance has been confirmed from animal studies and in vitro cell biology experiments[9,11,12] validating GP as an important target for structure based inhibitor design of new hypoglycemic agents.

The catalytic site of the enzyme is a deep cavity 15 Å from the protein surface accessible via a channel blocked by the inhibitor site and the 280s loop (residues 282–287). From T state to R state transition (activation of the enzyme), the 280s loop becomes disordered and displaced, opening this channel, allowing the entrance of the substrate and inducing the conformational change of a crucial residue, Arg569, to enter the catalytic site in place of Asp283 in order to create the phosphate recognition site.[8] Inhibition of glycogenolysis towards antidiabetic and other therapies has been reviewed recently, and updated information about glycogen phosphorylase is available, concerning in particular computations,[13] inhibitors binding at the active site[14,15] and the physiological control of liver glycogen metabolism studied in the light of novel glycogen phosphorylase inhibitors (GPis) .[16]

Within collaborative programs devoted to the design, synthesis, and evaluation by enzymology and crystallography of glucose-based molecules, we recently demonstrated that glucose-based motifs of the spirobicyclic or heterocyclic type (Fig. 1) are promising GPis, as when equipped with a 2-naphthyl substituent. The corresponding spiro-isoxazoline **A** (K_i = 0.63 μM),[17,18] spiro-oxathiazole **B** (K_i = 0.16 μM),[19,20] 3- (or 5)-*C*-β-D-glucopyranosyl-1,2,4-oxadiazoles, **C**[21] and **D**,[17] (K_i = 38 and 11.6 μM, respectively) [22] and *N*-benzoyl 1-(3-deoxy-3-fluoro-β-D-glucopyranosyl) cytosine **E** (K_i = 46.42 μM),[23] were to date among the best GPis known to bind at the enzyme catalytic site. We also reported on the synthesis, by multi-step efficient routes, of *C*-D-glucopyranosyl hydro-(and -1,4-benzo)quinones ultimately deacetylated to afford potentially active water-soluble materials.[24] Kinetic and crystallographic studies showed that **7** and **F** (Fig. 1) are competitive inhibitors of GP due to binding at the catalytic site, with K_i values found to be 0.9 and 1.3 mM for, respectively, 2-(β-D-glucopyranosyl)-hydroquinone and the corresponding 1,4-benzoquinone, while the 1,4-dimethoxy analog was not an inhibitor of GPb.[25] Annelation of dimethyl β-D-glucosyl-hydroquinones led to *C*-β-D-glucopyranosyl-chromanes and *C*-β-D-glucopyranosyl-vitamin E derivatives which showed interesting anti-oxidant properties.[26] Related *C*-glycosyl amino-substituted hydro- and benzoquinones were synthesized and evaluated for their antitumor activity.[27] Although weak inhibitors, the *C*-glucosyl hydro- and benzoquinones represented a new type of GPis, with a *C*-glycosidic bond resistant to hydrolysis and a six-membered ring amenable to structural modifications that might result in improved affinity for the enzyme. Introduction of substituents at the C-5 and C-6 positions of glucosyl hydroquinone (see Fig. 1 for numbering) was considered promising due to the proximity of the Asn284 side chain with the phenyl ring and the interactions observed by crystallography for these two carbon atoms with other residues of the enzyme (C-5 with N Asn284, C-6 with OD1 Asp283, and CB Leu136; see a reported discussion[25] in which the C-5 and C-6 carbons of the hydro/benzoquinone ring were numbered C-10 and C-11, as for the next structural studies). With our experience on the regioselective nitration of 2-(β-D-glucopyranosyl)-1,4-dimethoxy-benzene,[27] we synthesized C-5 or C-6 halogenated *C*-D-glucosyl hydroquinones and four of them were evaluated as GPis by kinetic experiments. Furthermore, to explore the molecular basis of their inhibition we have also determined the crystal structures of each of these four compounds in complex with GPb and the results are disclosed herein.

2. Materials and methods

2.1. Organic synthesis

2.1.1. General methods

Dichloromethane was washed three times with water, dried ($CaCl_2$), and distilled over CaH_2 before use. Other organic solvents were distilled. Thin-layer chromatography (TLC) was carried out on aluminium sheets coated with silica gel 60 F_{254} (Merck, Darmstadt, Germany). TLC plates were inspected under UV light (254, 312 nm), and/or developed by treatment with a mixture of 5% H_2SO_4 in EtOH followed by heating. Silica gel column chromatography was performed with Geduran® silica gel Si 60 (40–63 μm) purchased from Merck. ^1H and ^{13}C NMR spectra were recorded at 23 °C using Bruker AC200, DRX300 or DRX500 spectrometers with the residual solvent as the internal standard. The following abbreviations are used to indicate the observed multiplicities: s, singlet; d, doublet; dd, doublet of doublet; t, triplet; q, quadruplet; m, multiplet; br, broad. NMR solvents were purchased from Euriso-Top (Saint Aubin, France). HRMS (LSIMS) mass spectra were recorded in the positive mode (unless stated otherwise) using a Thermo Finnigan Mat 95 XL spectrometer. MS (ESI) mass spectra were

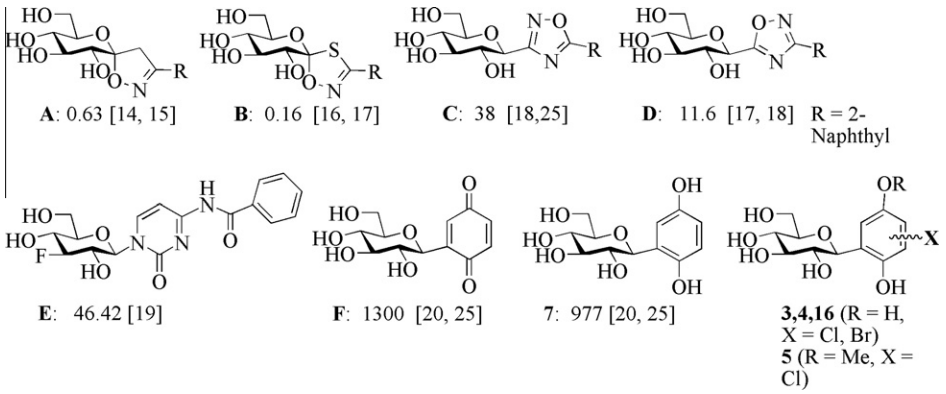

Figure 1. Recently reported inhibitors of GP, with their K_i values against RMGP*b* (μM) and new ones described herein.

recorded in the positive mode using a Thermo Finnigan LCQ spectrometer. Optical rotations were measured using a Perkin Elmer 241 polarimeter in a 1 dm cell. Compounds **1**, **2**, **5**, **6**, and **7** were obtained as described previously.[26]

2.1.2. 5-Chloro-2-(2,3,4,6-tetra-*O*-acetyl-β-D-glucopyranosyl)-1,4-dimethoxy-benzene (8) and 6-chloro-2-(2,3,4,6-tetra-*O*-acetyl-β-D-glucopyranosyl)-1,4-dimethoxy-benzene (10)

A mixture of compound **1** (637 mg, 1.36 mmol), *N*-chlorosuccinimide (254 mg, 1.91 mmol, 1.4 equiv) and NH_4NO_3 (21.8 mg, 0.272 mmol, 0.4 equiv) in dry CH_3CN (10 mL) was stirred at 60–65 °C for 3 h. As indicated by TLC, the starting material (R_f 0.29 petroleum ether/AcOEt 3:2) was totally converted into two more mobile compounds (R_f 0.31 and 0.34, respectively, petroleum ether/AcOEt 3:2, red-violet under UV 312 nm). The reaction mixture was poured into water (20 mL) and extracted with CH_2Cl_2 (3 × 20 mL). The extracts were combined and washed with brine, dried over $MgSO_4$, and evaporated. The residue was purified by chromatography (petroleum ether/AcOEt 4:1) on silica gel to afford pure compound **8** (633 mg, yield 93%) and compound **10** (12 mg, yield 1.5%).

2.1.2.1. Compound 8. White solid mp 110–112 °C (CH_2Cl_2/petroleum ether), $[\alpha]_D^{18}$ −16.2 (*c* 0.76 CH_2Cl_2); ^{1}H NMR (300.13 MHz, $CDCl_3$): δ 6.96 (s, 1H, Ar), 6.90 (s, 1H, Ar), 5.40–5.17 (m, 3H, H_2, H_3, H_4), 4.91 (d, 1H, $J_{1,2}$ = 9.5 Hz, H_1), 4.26 (dd, 1H, $J_{6,6'}$ = 12.4 Hz, $J_{5,6}$ = 4.8 Hz, H_6), 4.12 (dd, 1H, $J_{5,6'}$ = 2.3 Hz, $H_{6'}$), 3.86 (s, 3H, OMe), 3.79 (s, 3H, OMe), 3.88–3.75 (m, 1H, H_5), 2.06, 2.05, 2.00, 1.79 (4s, 12H, OAc); ^{13}C NMR (50 MHz, $CDCl_3$): δ 170.7 (C=O, acetyl), 170.3 (C=O, acetyl), 169.6 (C=O, acetyl), 169.1 (C=O, acetyl), 151.5 (C–OMe), 149.5 (C–OMe), 123.7 ($C_{arom.}$), 123.3 ($C_{arom.}$), 113.7 ($CH_{arom.}$), 112.2 ($CH_{arom.}$), 76.3, 74.5, 73.2, 71.8, 68.7 (C_1-C_5), 62.4 (C_6), 56.7 (OMe), 56.5 (OMe), 20.8, 20.7, 20.7, 20.4 (4 CH_3, acetyl); MS(CI) $C_{22}H_{27}ClO_{11}$: 503 (100%, ^{35}Cl), 505 (33%, ^{37}Cl) $[M+H]^+$.

2.1.2.2. Compound 10. Pale yellow oil, $[\alpha]_D^{20}$ −16.5 (*c* 3.2 CH_2Cl_2); ^{1}H NMR (300.14 MHz, $CDCl_3$): δ 6.92 (d, 1H, *J* = 3.0 Hz, Ar), 6.84 (d, 1H, Ar), 5.38 (t, 1H, $J_{2,3}$ = 6.9 Hz, H_2), 5.35 (t, 1H, $J_{3,4}$ = 6.9 Hz, H_3), 5.22 (m, 1H, H_4), 4.85 (br d, 1H, $J_{1,2}$ = ∼9.9 Hz, H_1), 4.25 (dd, 1H, $J_{5,6}$ = 5.1 Hz, $J_{6,6'}$ = 12.3 Hz, H_6), 4.11 (dd, 1H, $J_{5,6'}$ = 2.1 Hz, $H_{6'}$), 3.91–3.85 (m, 1H, H_5), 3.84 (s, 3H, OMe), 3.77 (s, 3H, OMe), 2.06, 2.06, 2.02, 1.82 (4s, 12H, OAc); ^{13}C NMR (50 MHz, $CDCl_3$): δ 170.7 (C=O, acetyl), 170.3 (C=O, acetyl), 169.6 (C=O, acetyl), 169.1 (C=O, acetyl), 156.1 (C–OMe), 148.5 (C–OMe), 131.2 ($C_{arom.}$), 128.4 ($C_{arom.}$), 117.1 ($CH_{arom.}$), 111.8 ($CH_{arom.}$), 76.4, 74.6, 74.3, 71.3, 68.7 (C_1-C_5), 62.4 (C_6), 61.9 (OMe), 55.8 (OMe), 20.8, 20.7, 20.7, 20.5 (4 CH_3, acetyl); HRMS-EI $M^{+\cdot}$ calcd for $C_{22}H_{27}ClO_{11}$: 502.1242; found 502.1241.

2.1.3. 5-Bromo-2-(2,3,4,6-tetra-*O*-acetyl-β-D-glucopyranosyl)-1,4-dimethoxy-benzene (9) and 6-bromo-2-(2,3,4,6-tetra-*O*-acetyl-β-D-glucopyranosyl)-1,4-dimethoxy-benzene (11)

A mixture of compound **1** (240 mg, 0.513 mmol), *N*-bromosuccinimide (147 mg, 0.821 mmol, 1.6 equiv) and NH_4NO_3 (16.5 mg, 0.205 mmol, 0.4 equiv) in dry CH_3CN (8 mL) was stirred at rt for about 3 h. TLC showed the starting material (R_f 0.42 petroleum ether/AcOEt 1:1) was completely converted into 2 more mobile compounds (R_f 0.46, 0.48, petroleum ether/AcOEt 1:1, red-violet under UV 312 nm). Water (15 mL) was added to the reaction mixture which was extracted with CH_2Cl_2 (3 × 15 mL). The extracts were combined, washed with brine, water, then dried over $MgSO_4$, and evaporated. The residue was purified by chromatography (petroleum ether/AcOEt 4:1) on silica gel to afford pure compounds **9**[28] (261 mg, 93% yield) and **11** (4.7 mg, 2% yield).

2.1.3.1. Compound 9. White solid; mp 118.5–120 °C (CH_2Cl_2/petroleum ether/Et_2O), $[\alpha]_D^{18}$ −19.4 (*c* 0.69 CH_2Cl_2); lit.[28] $[\alpha]_D^{18}$ −18.7 (*c* 1.0 CH_2Cl_2); ^{13}C NMR (50 MHz, $CDCl_3$): δ 170.7 (C=O, acetyl), 170.3 (C=O, acetyl), 169.6 (C=O, acetyl), 169.2 (C=O, acetyl), 151.7 (*C*–OMe), 150.5 (*C*–OMe), 124.5 ($C_{arom.}$), 116.7 ($CH_{arom.}$), 112.5 ($C_{arom.}$), 111.9 ($CH_{arom.}$), 76.3, 74.5, 73.3, 71.8, 68.8 (C_1–C_5), 62.4 (C_6), 56.9 (OMe), 56.6 (OMe), 20.8, 20.7, 20.7, 20.5 (4 CH_3, acetyl).

2.1.3.2. Compound 11. Pale yellow oil; ^{1}H NMR (300.14 MHz, $CDCl_3$): δ 7.08 (d, 1H, *J* = 3.0 Hz, Ar), 6.89 (d, 1H, Ar), 5.39 (t, 1H, $J_{3,4}$ = 9.3 Hz, H_3), 5.34 (t, 1H, $J_{2,3}$ = 9.3 Hz, H_2), 5.21 (m, 1H, H_4), 4.84 (br d, 1H, $J_{1,2}$ = ∼9.9 Hz, H_1), 4.24 (dd, 1H, $J_{5,6}$ = 5.1 Hz, $J_{6,6'}$ = 12.3 Hz, H_6), 4.12 (dd, 1H, $J_{5,6'}$ = 2.7 Hz, $H_{6'}$), 3.89 (m, 1H, H_5), 3.83 (s, 3H, OMe), 3.77 (s, 3H, OMe), 2.06, 2.06, 2.02, 1.82 (4s, 12H, OAc); ^{13}C NMR (75.5 MHz, $CDCl_3$): δ 171.0, 170.7, 169.9, 169.5 (4 C=O, acetyl), 156.7 (*C*–OMe), 150.0 (*C*–OMe), 131.5 ($C_{arom.}$), 120.4 ($CH_{arom.}$), 117.9 ($C_{arom.}$), 112.9 ($CH_{arom.}$), 76.8 (C_5), 74.9 (C_1 and C_2), 71.6 (C_3), 69.1 (C_4), 62.8 (C_6), 62.5 (OMe), 56.5 (OMe), 21.1, 21.1, 21.1, 20.9 (4 CH_3, acetyl); MS(CI) *m/z* (%): 547 (90%) $[^{79}Br+H]^+$, 549 (100%) $[^{81}Br+H]$; HRMS-CI: Calcd for $C_{22}H_{28}BrO_{11}$ $[M+H]^+$: 547.0815. Found: 547.0815.

2.1.4. 5-Chloro-2-(2,3,4,6-tetra-*O*-acetyl-β-D-glucopyranosyl)-1,4-benzoquinone (12)

2.1.4.1. Prepared from 8. Compound **8** (256 mg, 0.508 mmol) dissolved in CH_3CN (2 mL) was reacted with CAN (1.02 g, 2.03 mmol, 4 equiv) dissolved in water (5 mL). After stirring the mixture for 2 h at rt, TLC showed the complete conversion of compound **8**, in favor of compound **12** only (R_f 0.48 petroleum ether/AcOEt 5:4 red-violet under UV 312 nm, black under UV 254 nm). Water (10 mL) was poured into the reaction mixture which was extracted with CH_2Cl_2 (3 × 15 mL). The extracts were combined and washed with brine, water, dried over $MgSO_4$, and concentrated. Chromatography of residue on silica gel with petroleum ether/AcOEt 3/2 led to pure **12** (172 mg, 95% yield).

2.1.4.2. Prepared from 14. 5-Chloro-2-(2,3,4,6-tetra-*O*-acetyl-β-D-glucopyranosyl)-hydroquinone (**14**) [prepared from **2** (285 mg, 0.6 mmol) and $(CH_3)_3SiCl$—vide infra] was dissolved in $CHCl_3$. Freshly prepared Ag_2O (1.18 g, 5.1 mmol, 8.5 equiv) was added by small portions while stirring the mixture at rt. TLC indicated the complete conversion of the starting material into a more mobile product after 3 h (R_f = 0.59 petroleum ether/AcOEt 3:2). After removal of the solids by filtration, the solvent was evaporated under reduced pressure. The residue was purified by chromatography (petroleum ether/AcOEt 2:1) on silica gel to afford **12** (221 mg, 78% yield).

2.1.4.3. Compound 12. Golden-yellow solid, mp 101–102 °C (CH_2Cl_2/petroleum ether); R_f = 0.59 (petroleum ether/AcOEt 3:2 red-violet under UV 312 nm, black under UV 254 nm); $[\alpha]_D^{19}$ −40.7 (c 0.78 CH_2Cl_2); ^{1}H NMR (300.13 MHz, $CDCl_3$:) δ 7.03 (s, 1H, Ar), 6.98 (s, 1H, Ar), 5.36 (t, 1H, $J_{3,4}$ = 9.3 Hz, H_3), 5.13 (t, 1H, $J_{4,5}$ = 9.6 Hz, H_4), 4.94 (t, 1H, $J_{2,3}$ = 9.6 Hz, H_2), 4.61 (d, 1H, $J_{1,2}$ = 9.9 Hz, H_1), 4.24 (dd, 1H, $J_{5,6}$ = 4.8 Hz, $J_{6,6'}$ = 12.3 Hz, H_6), 4.12 (dd, 1H, $J_{5,6'}$ = 2.1 Hz, $H_{6'}$), 3.80 (ddd, 1H, H_5), 2.09, 2.05, 2.01, 1.91 (4 s, 12H, OAc); ^{13}C NMR (50 MHz, $CDCl_3$): δ 183.5 (C=O, benzoquinone), 179.2 (C=O, benzoquinone), 170.6 (C=O, acetyl), 170.0 (C=O, acetyl), 169.9 (C=O, acetyl), 169.5 (C=O, acetyl), 144.9 ($C_{quin.}$), 144.2 ($C_{quin.}$), 133.4 ($CH_{quin.}$), 133.3 ($CH_{quin.}$), 76.3, 73.5, 72.6, 72.0, 68.2 (C_1–C_5), 62.0 (C_6), 20.8 (CH_3, acetyl), 20.6 (CH_3, acetyl), 20.6 (CH_3, acetyl), 20.5 (CH_3, acetyl); MS (ESI) 495.0 (100%), 497.0 (43%) $[M+23]^+$; MS (CI) $[M+H]^+$ 473; HRMS (CI): Calcd for $C_{20}H_{22}O_{11}Cl$ $[M+H]^+$ 473.0851. Found: 473.0852.

2.1.5. 5-Bromo-2-(2,3,4,6-tetra-*O*-acetyl-β-D-glucopyranosyl)-1,4-benzoquinone (13)

Compound **13** was prepared by CAN oxidation of **9** in 90% yield as for synthesis of **12**. Compound **13**: golden-yellow solid, mp 141–142 °C (CH_2Cl_2/petroleum ether), $[\alpha]_D^{20}$ −40.0 (*c* 0.66 CH_2Cl_2); ^{1}H NMR (300.13 MHz, $CDCl_3$): δ 7.28 (s, 1H, Ar), 7.09 (s, 1H, Ar), 5.37 (t, 1H, $J_{3,4}$ = 9.3 Hz, H_3), 5.14 (t, 1H, $J_{4,5}$ = 9.6 Hz, H_4), 4.95 (t, 1H, $J_{2,3}$ = 9.3 Hz, H_2), 4.61 (d, 1H, $J_{1,2}$ = 9.9 Hz, H_1), 4.26 (dd, 1H, $J_{5,6}$ = 4.8 Hz, $J_{6,6'}$ = 12.6 Hz, H_6), 4.14 (dd, 1H, $J_{5,6'}$ = 2.1 Hz, $H_{6'}$), 3.81 (ddd, 1H, H_5), 2.11, 2.06, 2.03, 1.93 (4 s, 12H, OAc); ^{13}C NMR (50 MHz, $CDCl_3$): δ 183.1 (C=O, benzoquinone), 179.1 (C=O, benzoquinone), 170.6 (C=O, acetyl), 170.0 (C=O, acetyl), 169.9 (C=O, acetyl), 169.5 (C=O, acetyl), 144.8 ($C_{quin.}$), 137.8 ($CH_{quin.}$), 137.6 ($C_{quin.}$), 133.1 ($CH_{quin.}$), 76.3, 73.5, 72.6, 72.0, 68.2 (C_1–C_5), 62.0 (C_6), 20.8, 20.6, 20.6, 20.5 (4 CH_3, acetyl); MS ($^+$c ESI) for $C_{20}H_{21}O_{11}Br$: 456.8 (^{79}Br) and 458.8 (^{81}Br) [M+H−CH_3COOH]$^+$, 516.7 [M+H]$^+$, 538.9 (^{79}Br) and 541.0 (^{81}Br) [M+Na]$^+$.

2.1.6. 5-Chloro-2-(2,3,4,6-tetra-*O*-acetyl-β-D-glucopyranosyl)-hydroquinone (14)

2.1.6.1. Prepared from 12. A freshly prepared aqueous solution (4 mL) of $Na_2S_2O_4$ (85% tech., 222 mg, 1.27 mmol, 6 equiv) was introduced in a flask containing a solution of compound **12** (100 mg, 0.212 mmol) in 5 mL $CHCl_3$. After the mixture was stirred vigorously for 40 min at rt, TLC showed compound **12** (R_f 0.60, petroleum ether/AcOEt 1:1 red-violet under UV 312 nm, dark spot under UV 254 nm) was completely converted into a more polar compound (R_f 0.37, petroleum ether/AcOEt 1:1 red-violet under UV 312 nm). After extracting the reaction mixture with $CHCl_3$ (3 × 15 mL), the combined organic phase was washed with brine, water, and dried over $MgSO_4$. After filtration and concentration, the residue was purified by chromatography (petroleum ether/AcOEt 3:2) on silica gel to afford pure compound **14** (88 mg, 88% yield).

2.1.6.2. Prepared from 2. Neat chlorotrimethylsilane $(CH_3)_3$ SiCl (0.15 mL, 1.2 mmol, 1.5 equiv) and $BF_3{\cdot}Et_2O$ (0.01 mL, 0.08 mmol, 0.1 equiv) were successively added to a stirred solution of 2-(2,3,4,6-tetra-*O*-acetyl-β-D-glucopyranosyl)-1,4-benzoquinone (**2**, 350 mg, 0.8 mmol) in 10 mL CH_3CN. TLC showed that the starting material was completely transformed into a more polar product within 14 h. After quenching by addition of water (15 mL), the reaction mixture was extracted with CH_2Cl_2 (3 × 15 mL). The extracts were combined, washed with brine, dried ($MgSO_4$), and evaporated. The residue was purified by chromatography (petroleum ether/AcOEt 7:3) on silica gel to afford pure **14** (318 mg, 84% yield). See below for another access from **2** to **14** and **18** as, respectively, the minor and major products.

2.1.6.3. Compound 14. White solid, mp 165–166 °C (not recrystallized); R_f = 0.20 (petroleum ether/AcOEt 2:1); $[\alpha]_D^{21}$ −33.1 (*c* 0.66 CH_2Cl_2); ^{1}H NMR (300.14 MHz, $CDCl_3$): δ 6.89 (s, 1H, Ar), 6.74 (br s, 1H, OH exchangeable with D_2O), 6.69 (s, 1H, Ar), 5.35–5.23 (m, 3H, H_2, H_3, H_4), 5.17 (br s, OH exchangeable with D_2O), 4.53 (d, 1H, $J_{1,2}$ = 9.2 Hz, H_1), 4.33 (dd, 1H, $J_{5,6}$ = 3.6 Hz, $J_{6,6'}$ = 12.6 Hz, H_6), 4.17 (dd, 1H, $J_{5,6'}$ = 2.2 Hz, $H_{6'}$), 3.88 (ddd, 1H, $J_{4,5}$ = 9.3 Hz, H_5), 2.12, 2.07, 2.01, 1.89 (4 s, 12H, OAc); ^{13}C NMR (50.32 MHz, $CDCl_3$): δ 170.7, 170.4, 169.4, 168.9 (4 C=O, acetyl), 148.9 (C-OH), 144.8 (C-OH), 121.0 ($C_{arom.}$), 120.9 ($C_{arom.}$), 118.1 ($CH_{arom.}$), 115.5 ($CH_{arom.}$), 79.4, 76.2, 73.6, 70.6, 67.8 (C_1-C_5), 61.5 (C_6), 20.7, 20.7, 20.6, 20.5 (4 CH_3, acetyl); MS ($^+$c ESI): 474.8 [M+H]$^+$; 491.9 [M+NH_4]$^+$; 497.0 [M+Na]$^+$; 970.5, 972.6 [2 M+Na]$^+$; MS ($^-$c ESI): 472.8: [M−H]$^-$; 508.9 [M+Cl]$^-$; 946.7 [2M−H]$^-$; HRMS-CI: Calcd for $C_{20}H_{24}ClO_{11}$ [M+H] 473.1214. Found: 473.1211.

2.1.7. 5-Bromo-2-(2,3,4,6-tetra-*O*-acetyl-β-D-glucopyranosyl)-hydroquinone (15)

A freshly prepared aqueous solution (6 mL) of $Na_2S_2O_4$ (85% tech., 349 mg, 2.01 mmol, 6 equiv) was introduced in a flask containing compound **13** (173 mg, 0.335 mmol) dissolved in 5 mL $CHCl_3$. The reaction mixture was stirred vigorously at rt. After 80 min, TLC showed compound **13** (R_f 0.60, petroleum ether/THF 3:2 red-violet under UV 312 nm, dark spot under UV 254 nm) was changed into a more polar compound (R_f 0.37, petroleum ether/THF 3:2 red-violet under UV 312 nm). The reaction mixture was extracted with $CHCl_3$ (3 × 15 mL), washed with brine, water, dried over $MgSO_4$. After filtration and concentration, the residue was purified by chromatography (petroleum ether/AcOEt 3:2) on silica gel to afford pure compound **15** (162 mg, 93% yield).

2.1.7.1. Compound 15. White solid, mp 155–156 °C; $[\alpha]_D^{23}$ −32.7 (*c* 0.7 CH_2Cl_2); ^{1}H NMR (300.13 MHz, $CDCl_3$) δ 7.03 (s, 1H, Ar), 6.68 (s, 1H, exchangeable with D_2O, OH), 6.68 (s, 1H, Ar), 5.33 (t, 1H, $J_{3,4}$ = 9.0 Hz, H_3), 5.26 (t, 1H, $J_{2,3}$ = 9.6 Hz, H_2), 5.24 (t, 1H, $J_{4,5}$ = 9.6 Hz, H_4), 5.17 (s, 1H, exchangeable with D_2O, OH), 4.52 (d, 1H, $J_{1,2}$ = 9.3 Hz, H_1), 4.32 (dd, 1H, $J_{5,6}$ = 3.6 Hz, $J_{6,6'}$ = 12.6 Hz, H_6), 4.16 (dd, 1H, $J_{5,6'}$ = 2.1 Hz, $H_{6'}$), 3.87 (dq, 1H, H_5), 2.12, 2.06, 2.01, 1.88 (4s, 12H, OAc); ^{13}C NMR (50 MHz, $CDCl_3$): δ 170.7, 170.4, 169.5, 168.9 (4 C=O, acetyl), 149.0 (C–OH), 145.9 (C-OH), 121.7 ($C_{arom.}$), 120.9 ($CH_{arom.}$), 115.2 ($CH_{arom.}$), 111.0 ($C_{arom.}$), 79.2, 76.2, 73.6, 70.6, 67.9 (C_1–C_5), 61.6 (C_6), 20.7, 20.7, 20.6, 20.5 (4 CH_3, acetyl); MS-CI: *m/z*: 519, 521 [M+H]$^+$; HRMS-CI: Calcd for $C_{20}H_{24}BrO_{11}$ [M+H] 519.0502. Found: 519.05045.

2.1.8. 6-Chloro-2-(2,3,4,6-tetra-*O*-acetyl-β-D-glucopyranosyl)-hydroquinone (18)

2.1.8.1. Prepared from 2. Compound **2** (169 mg, 0.386 mmol) was dissolved in 15 mL dry THF. Then freshly distilled AcCl (110 μL, 1.54 mmol, 4 equiv) and water (0.3 mL) were successively added to the above solution. After 6 h, TLC showed that compound **2** (R_f 0.60, petroleum ether/AcOEt 1:1 red-violet under UV 312 nm, dark spot under UV 254 nm) almost disappeared while four more polar spots became visible on the plates. After adding more water (5 mL), the mixture was extracted with CH_2Cl_2 (3 × 15 mL) and the combined organic phase was washed with brine, water, and dried over $MgSO_4$. After filtration and concentration, the residue was purified by chromatography (petroleum ether/AcOEt 5:2) on silica gel to afford **14** (45 mg, 24% yield) and **18** (109 mg, 60% yield).

2.1.8.2. Prepared from 10. In another route, as compound **10** was only partially converted (∼10%) to **17** upon oxidation with CAN (10 equiv, two days), this mixture was treated with aqueous $Na_2S_2O_4$ to afford, after separation on column of unreacted **10**, a low amount of **18** (7 mg).

2.1.8.3. Compound 18. Colorless oil, R_f = 0.46 (petroleum ether/AcOEt 1:1 red-violet under UV 312 nm); $[\alpha]_D^{20}$ −15.7 (*c* 1.10, $CHCl_3$); ^{1}H NMR (500 MHz, $CDCl_3$): δ 6.83 (d, 1H, *J* = 2.8 Hz, Ar), 6.69 (d, 1H, *J* = 2.8 Hz, Ar), 5.90 (br s, 1H, OH), 5.37 (t, 1H, *J* = 9.4 Hz), 5.23 (q, 2H, *J* = 9.7 Hz), 4.81 (d, 1H, $J_{1,2}$ = 9.9 Hz, H_1), 4.30 (dd, 1H, $J_{5,6}$ = 4.5 Hz, $J_{6,6'}$ = 12.5 Hz, H_6), 4.15 (m, 2H, OH, $H_{6'}$), 3.88 (m, 1H, $J_{4,5}$ = 10 Hz, $J_{5,6}$ = 4.5 Hz, $J_{5,6'}$ = 2 Hz, H_5), 2.09, 2.06, 2.01, 1.86 (4s, 12H, OAc); ^{13}C NMR (75 MHz, $CDCl_3$) δ 170.9, 170.5, 169.7, 169.3 (4 C=O, acetyl), 149.4, 143.6 (2 C–OH), 123.5, 120.9, 116.9, 113.8 (4 C, Ar), 76.1, 75.6, 74.0, 71.6, 68.3 (C_1–C_5), 62.0 (C6), 20.7, 20.6, 20.6, 20.4 (4 CH_3, acetyl); MS(ESI+) *m/z* (%):475.1 (25) [M]$^+$, 497.1 (100) and 499.1 (32) [M+Na]$^+$, 1116.6 [2 M+Na]$^+$; HRMS(E-SI+) *m/z*: Calcd for [M+Na]$^+$ $C_{20}H_{23}Na_1Cl_1O_{11}$: 497.0827. Found: 497.0821.

2.1.9. 5-Chloro-2-(β-D-glucopyranosyl)-hydroquinone (3)

2.1.9.1. Prepared by acid-catalyzed deacetylation of 14. 2-(2,3,4,6-Tetra-*O*-acetyl-β-D-glucopyranosyl)-5-chloro-1,4-hydroquinone (**14**) (142 mg, 0.30 mmol) was dissolved in 10 mL dry CH_3OH. AcCl (61 μL, 0.86 mmol, 2.9 equiv) was added to the solution. The mixture protected from light was stirred at rt under argon for six days, whereupon TLC showed that the starting material (R_f 0.37 petroleum ether/AcOEt 1:1 red-violet under UV 312 nm) was converted into a new very polar product (R_f 0.24 CH_2Cl_2/CH_3OH 4:1, red-violet under UV 312 nm). After concentration under vacuum, the residue was purified by chromatography (CH_2Cl_2/CH_3OH 10:1) on silica gel to afford **3** (85 mg, 93% yield).

2.1.9.2. Prepared by base-catalyzed deacetylation of 14. 2-(2,3,4,6-Tetra-*O*-acetyl-β-D-glucopyranosyl)-5-chloro-1,4-hydroquinone **14** (100 mg, 0.21 mmol) was dissolved in 8 mL dry CH_3OH. A solution of CH_3ONa in methanol (0.1 M, 4.2 mL) was added under argon. After the reaction mixture was stirred at rt for 2 h, TLC showed compound **14** changed into a more polar compound (R_f 0.24 CH_2Cl_2/CH_3OH 4:1, red-violet under UV 312 nm). Then Dowex 50wX2 (H^+) ion-exchange resin was cautiously added to the reaction mixture, so as to reach pH ~6 (litmus paper). Without delay, the resin was removed by filtration and after concentration, the residue was applied to a short column (CH_2Cl_2/CH_3OH 10:1) to afford compound **3** (62 mg, 96% yield).

2.1.9.3. Prepared by acid-catalyzed deacetylation of 2. After compound **2** (252 mg, 0.575 mmol) was dissolved in 10 mL MeOH, freshly distilled AcCl (1 mL, 25 equiv) was added via a syringe into the above mixture (9% v/v AcCl in MeOH). At once, the color of the solution changed from orange to almost colorless. After the mixture was stirred at rt for 30 h, TLC showed the starting material was converted to more polar deacetylated compounds giving two spots (R_f 0.55 and 0.18, MeOH/CH_2Cl_2 1:4). The volatiles were evaporated under reduced pressure. The residue was applied to a column of chromatography on silica gel (MeOH/CH_2Cl_2 1:10) to afford compound **5** (18 mg, 0.06 mmol, 10.4% yield) ,[25] and the inseparable mixture of **3** and **4** (82 mg, 46.7% yield, **3**/**4** ratio: ~65:35), as a glassy yellow solid, R_f 0.18, MeOH/CH_2Cl_2 1:4. A similar experiment with 100 mg of **2** confirmed these results. In another experiment, compound **2** (90 mg, 0.205 mmol) dissolved in MeOH (10 mL) was deacetylated with AcCl (1.5 mL, 100 equiv) upon stirring for 30 h at rt to afford 41 mg (65% yield) of **3** and **4**, with no detectable amount of **5**.

2.1.9.4. Compound 3 $[\alpha]_D^{22}$ +14.4 (*c* 0.8 CH_3OH); ^1H NMR (200 MHz, D_2O) δ 7.04 (s, 1H, Ar), 7.02 (s, 1H, Ar), 4.64 (d, 1H, $J_{1,2}$ = 8.8 Hz, H_1), 3.95–3.60 (m, 6H, H_2, H_3, H_4, H_5, H_6, $H_{6'}$); ^{13}C NMR (50.32 MHz, D_2O) δ 148.7 (C-OH), 145.5 (C-OH), 124.7 ($C_{arom.}$), 121.5 ($C_{arom.}$), 118.0 ($CH_{arom.}$), 116.8 ($CH_{arom.}$), 80.7, 77.9, 76.2, 73.7, 70.2 (C_1-C_5), 61.3 (C_6); MS FAB negative mode: 305 $[M-H]^-$; HRMS (LSIMS): Calcd for $C_{12}H_{14}ClO_7$ $[M-H]^-$: 305.0428. Found: 305.0435.

2.1.10. 6-Chloro-2-(β-D-glucopyranosyl)-hydroquinone (4)

Compound **18** (96 mg, 0.202 mmol) was dissolved in 6 mL dry CH_3OH. AcCl (0.805 mmol, 4 equiv) was added to the solution. The mixture protected from light was stirred at rt under argon for four days. TLC showed that the starting material (R_f 0.46 petroleum ether/AcOEt 1:1 red-violet under UV 312 nm) was converted into a new polar product (R_f 0.20 CH_2Cl_2/CH_3OH 4:1, red-violet under UV 312 nm). After concentration under vacuum, the residue was purified by chromatography (CH_2Cl_2/CH_3OH 15:1) on silica gel to afford pure compound **4** (57 mg, 92% yield). $[\alpha]_D^{20}$ +27.2 (*c* 0.8, CH_3OH); ^1H NMR (500 MHz, D_2O): δ 6.93 (d, 1H, *J* = 2.9 Hz, Ar), 6.81 (d, 1H, Ar), 4.64 (d, 1H, *J* = 9.3 Hz, H_1), 3.84 (d, 1H, *J* = 12.2 Hz, H_6), 3.73 (dd, 1H, *J* = 3.2, 12.4 Hz, $H_{6'}$), 3.65–3.52 (m, 4H, H_2, H_3, H_4, H_5); ^{13}C NMR (100.6 MHz, CD_3OD) δ 150.5, 143.6 (2 C–OH), 128.9, 121.7, 115.3, 113.4 (4 C, Ar), 80.9, 78.4, 77.0, 74.8, 70.2 (C_1–C_5), 61.5 (C6); ^{13}C NMR (50.32 MHz, D_2O) δ 150.0, 143.9 (2 C–OH), 128.1, 123.0, 117.2, 114.4 (4 C, Ar), 80.6, 77.8, 76.9, 73.9, 70.1 (C_1–C_5), 61.2 (C6); MS(ESI+) *m*/*z* (%): $[M+Na]^+$ 329.0 (100), $[M+Na]^+$ 331.0 (30); HRMS (ESI+) *m*/*z*: Calcd for $[M+Na]^+$ $C_{12}H_{15}Na_1Cl_1O_7$: 329.0404. Found: 329.0408.

2.1.11. 5-Bromo-2-(β-D-glucopyranosyl)-1,4-hydroquinone (16)

After compound **15** (127 mg, 0.245 mmol) was dissolved in 10 mL dry CH_3OH, AcCl (50 μL, 0.49 mmol, 2 equiv) was added to the solution. The mixture protected from light was stirred at rt under argon for six days. TLC showed that the starting material (R_f 0.34 petroleum ether/AcOEt 1:1 red-violet under UV 312 nm) was converted into a new polar product (R_f 0.24 CH_2Cl_2/CH_3OH 4:1, red-violet under UV 312 nm). After concentration under vacuum, the residue was purified by chromatography (CH_2Cl_2/CH_3OH 10:1) on silica gel to afford compound **16** (82 mg, 95% yield).

2.1.11.1. Compound 16. White foam. $[\alpha]_D^{20}$ +3.4 (*c* 1 CH_3OH); ^1H NMR (300.13 MHz, D_2O) δ 7.09 (s, 1H, Ar), 6.95 (s, 1H, Ar), 4.55 (d, 1H, $J_{1,2}$ = 9.3 Hz, H_1), 3.82 (dd, 1H, $J_{5,6}$ = 1.2 Hz, $J_{6,6'}$ = 12 Hz, H_6), 3.72 (dd, 1H, $J_{5,6'}$ = 4.2 Hz, $H_{6'}$), 3.64–3.50 (m, 4H, H_2, H_3, H_4, H_5); ^{13}C NMR (50.32 MHz, D_2O) δ 148.8 (C–OH), 146.6 (C–OH), 125.4 ($C_{arom.}$), 120.9 ($CH_{arom.}$), 116.4 ($CH_{arom.}$), 110.5 ($C_{arom.}$), 80.6, 77.9, 76.3, 73.7, 70.1 (C_1–C_5), 61.2 (C6); MS ESI $^+$c: 373, 375 1:1 ratio $[M+Na]^+$; 722.7, 724.6, 726.8 1:2:1 ratio $[2M+Na]^+$; MS ESI $^-$c: 349.0, 351 1:1 ratio $[M-H]^-$; 386.8 $[M+Cl]^-$; 734,6, 736.6, 738.6 $[2M+Cl]^-$; HRMS-LSIMS: Calcd for $C_{12}H_{14}BrO_7$ $[M-H]^-$ 348.9923. Found: 348.9920.

2.2. Enzyme isolation and kinetic experiments

Glycogen phosphorylase (GPb) was isolated from rabbit skeletal muscle and purified as described previously.[29] Kinetic studies were performed in the direction of glycogen synthesis with 5 μg/ml enzyme, constant concentrations of glycogen (0.2% w/v), Glc-1-P (2 mM), AMP (1 mM) and various concentrations of inhibitors. They were carried out in the presence of 30 mM imidazole/HCl buffer 60 mM KCl, 0.6 mM EDTA, and 0.6 mM dithiothreitol (pH 6.8). Experiments were performed in the presence of 1% or 2% DMSO and the K_m of the enzyme was 2.1–2.6 mM. Enzyme activity was measured at pH 6.8 by the release of inorganic phosphate as described previously.[30]

2.3. X-ray crystallography

GPb crystals, grown in the tetragonal lattice, space group $P4_32_12$, as previously described[31] were soaked with 100 mM of a mixture of **3** and **4** (21 h), 10 mM of **5** (2.5 h), 20 mM of **16** (6 h), or 70.1 mM of **3** (20 h) in a solution of the crystallization media prior to data collection. Diffraction data were collected at the Daresbury Synchrotron Radiation Source, UK and at the EMBL Hamburg Outstation, Germany. Data reduction and integration followed by scalling and merging of the intensities obtained was performed with the HKL program suite.[32] Crystallographic refinement of the complexes was performed by maximum-likelihood methods using REFMAC.[33] The starting model employed for the refinement of the complexes was the structure of the native T state GPb complex determined at 1.9 Å resolution (Leonidas et al., unpublished results). Ligand models of the compounds were fitted to the electron density maps after adjustment of their torsion angles. Alternate cycles of manual rebuilding with COOT[34] and refinement with REFMAC improved the quality of the models. The stereochemistry of the protein residues was validated by PROCHECK.[35] Hydrogen bonds and van der Waals interactions were calculated with the

program CONTACT as implemented in CCP4[36] applying a distance cut off of 3.3 and 4.0 Å, respectively. Protein structures were superimposed using LSQKAB as implemented in CCP4.[36] Figures were prepared with the programs MolScript[37] and PyMol[38] rendered with Raster3D.[39] The coordinates of the new structures have been deposited with the RCSB Protein Data Bank (http://www.rcsb.org/pdb) with codes 3NP7 (mixture of **3** and **4**), 3NP9 (**5**), 3NPA (**16**) and 3S0J (**3**).

3. Results and discussion

3.1. Organic synthesis

Tetra-*O*-acetyl-β-D-glucopyranosyl-1,4-dimethoxybenzene **1** (the numbering shown in Scheme 1 is used for discussing the syntheses and for the compounds' names in the Experimental section), prepared in good yield from penta-*O*-acetyl-β-D-glucopyranose and 1,4-dimethoxybenzene[28] was oxidized with ceric ammonium nitrate (CAN) in aqueous acetonitrile to afford β-D-glucopyranosyl-1,4-benzoquinone **2**, isolated as moderately stable yellow needles in almost quantitative yield.[24,25] Acid-catalyzed deacetylation of **2** (MeOH containing acetyl chloride, 25/100 equiv) led by addition of hydrochloric acid and complete deacetylation, to **3** and **4** inseparable in our hand (46–65% total yield, ratio: ~65:35), and to **5** formed in less than 10–12% yield. The major isomer **3** displayed a chlorine atom at the C-5 position (Scheme 1), *para* related to the sugar substituent, showing an addition regioselectivity already observed when 2-(β-D-glucopyranosylthio)-1,4-benzoquinone was treated with HCl in $CHCl_3$.[40] To our surprise, when deacetylation was carried out with lower amounts of AcCl in MeOH, **2** was converted cleanly within one week to **5** (80% yield) which displayed a methoxy group at the C-4 position.[25] As reduction of **2** to hydroquinone **6** was straightforward as was its deacetylation to **7** under either acid or base-catalyzed conditions,[25] another route to the target compounds could be followed. Compound **1** was halogenated by either *N*-chlorosuccinimide (NCS) [41] or *N*-bromosuccinimide (NBS) [42] with NH_4NO_3 as catalyst[41,43] affording **8**[27] and **9** (C-5 chloro and bromo isomers) both in 93% yield, and trace amount of the C-6 halogenated regioisomers **10** (chloro) and **11** (bromo). Upon treatment with CAN in aqueous CH_3CN, compounds **8** and **9** were oxidized to the corresponding 1,4-benzoquinones **12** and **13** obtained in high yield. Equally high yielding was their $Na_2S_2O_4$-mediated reduction to the corresponding hydroquinones **14** and **15.** These were deacetylated in good yields under acid-catalyzed conditions (cat. AcCl in MeOH), while deacetylation under Zemplén conditions (MeONa in MeOH) proved less reproducible, with formation of unidentified byproducts. In contrast, the minor C-6 halogenated isomers **10** and **11** could not be transformed efficiently into benzoquinones because of scarcity and also due to their higher stability: treatment of **10** with CAN resulted in a ~10% conversion only, to produce low amounts of **17**. As **10** and **17** had a similar mobility on TLC plates, separation of **17** was not attempted, and the mixture from oxidation was subjected to reduction with $Na_2S_2O_4$. The more polar 6-chloro-hydroquinone **18** was easily separated from the starting material **10**. However, the obtained amount (7 mg) was so low that synthesizing **18** by another route was needed. In agreement with earlier data,[44] we observed that treatment of the glycosyl benzoquinone **2** with

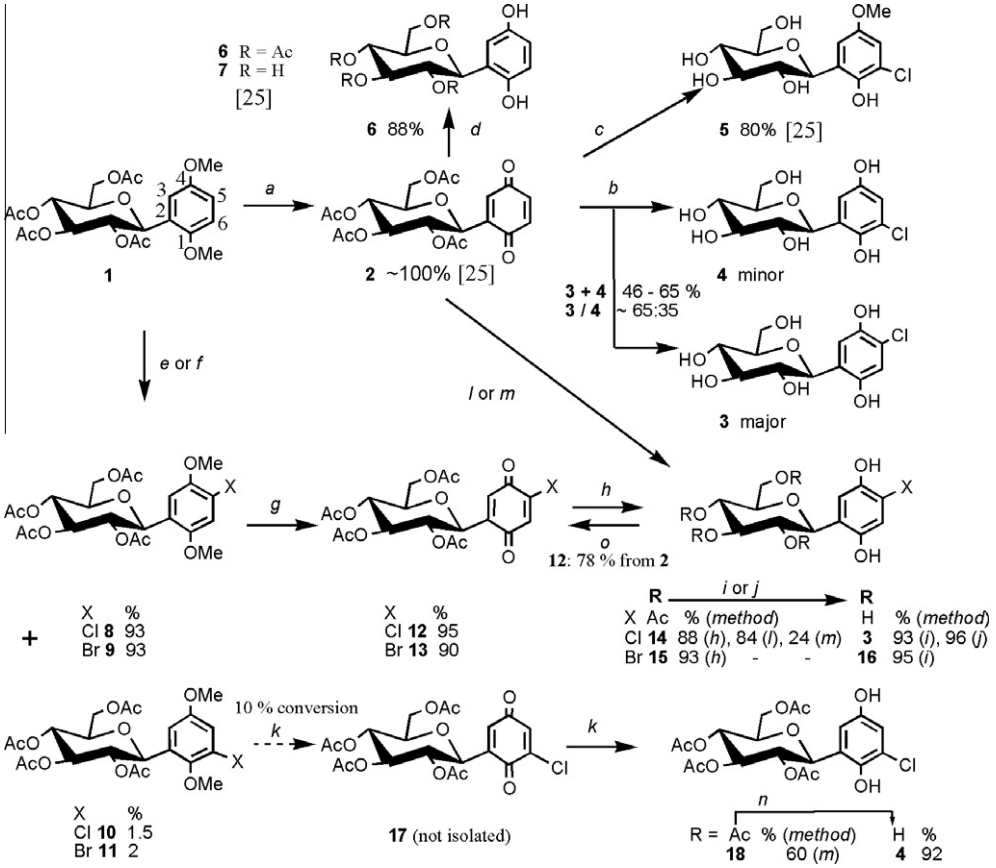

Scheme 1. Synthetic routes to halogenated β-D-glucopyranosyl hydroquinone regioisomers. Reagents conditions: (*a*) CAN (3 equiv), CH_3CN/H_2O, 1:1 or 2:3; (*b*) MeOH, AcCl (25–100 equiv), 30 h; (*c*) MeOH, AcCl (~3.3 equiv), eight days; (*d*) $NaBH_4$ (2 equiv), EtOAc, rt, 30 min; (*e*) CH_3CN, NCS (1.4 equiv), NH_4NO_3 (0.4 equiv), 60–65 °C, 3 h; (*f*) CH_3CN, NBS (1.6 equiv), NH_4NO_3 (0.4 equiv), rt, 3 h; (*g*) CAN (4 equiv), CH_3CN/H_2O 2:5, rt, 2 h; (*h*) $Na_2S_2O_4$ (6 equiv), $CHCl_3/H_2O$, rt; (*i*) MeOH, AcCl (2.0–2.9 equiv), rt, six days; (*j*) catal. MeONa in MeOH, rt, 2 h; (*k*) (a) CAN (10 equiv), CH_3CN/H_2O, two days, 10% conversion of **10**; b) $Na_2S_2O_4$ (6 equiv), $CHCl_3/H_2O$, **18** (7 mg); (*l*) CH_3CN, Me_3SiCl (1.5 equiv), $BF_3{\cdot}OEt_2$ (0.1 equiv), rt, 14 h; (*m*) THF/H_2O, AcCl (4 equiv), 6 h; (*n*) MeOH, AcCl (4 equiv), rt, four days; (*o*) $CHCl_3$, Ag_2O (8.5 equiv), rt, 3 h.

chlorotrimethylsilane Me_3SiCl in the presence of $BF_3{\cdot}Et_2O$ in CH_3CN afforded cleanly the corresponding C-5 chlorinated hydroquinone **14** already obtained by another route. We reasoned that the C-6 halogenated hydroquinone could be produced under conditions similar to those applied for the synthesis of the C-6 chlorinated compound **5**. To our delight, the glycosyl benzoquinone **2**, when treated with AcCl in THF/H_2O, gave easily separable C-5 and C-6 chlorinated hydroquinones **14** and **18** in 24 and 60% isolated yield, respectively. Finally, acid-catalyzed deacetylation (MeOH containing 0.5% AcCl, rt) proved to be efficient, so the desired compounds **3** and **4** were obtained in high yield and sufficient quantity for further tests. The halogenation pattern of the prepared compounds was established easily by ^{1}H NMR spectroscopy. In case of C-5 substitution, the two *para* related protons of the phenyl or 1,4-benzoquinone ring appeared both as singlet ($J_{para} = \sim 0$ Hz), while the *meta* related counterparts associated to the C-6 halogenation gave two doublets ($J_{meta} = \sim 3$ Hz). In the ^{1}H NMR spectra of **8** and **9** recorded at 300 MHz, signals for H-1 appeared as doublet as expected, but for **10** and **11**, the H-1 signals were more complex, suggesting the existence of conformers due to a restricted rotation of the C-glycosidic bond, as already observed for related dimethyl *meta*-substituted analogs.[26]

3.2. Enzyme kinetics

The inhibitory efficiency of three hydroquinone derivatives (**3**, **5**, **16**) was tested in kinetic experiments with rabbit muscle glycogen phosphorylase b (GPb) while it was estimated for one (**4**) and their inhibitory constants (IC_{50}, Table 1) are compared to that of **7**, as a reference. All compounds displayed competitive inhibition with respect to Glc-1-P, at constant concentrations of glycogen (0.2% w/v), AMP (1 mM) and Glc-1-P (2 mM). Kinetic experiments were carried out in the direction of glycogen synthesis and IC_{50} values obtained are in the μM range. The lead compound **7** displays a K_i of 0.9 mM[25] and it is a slightly better inhibitor than α-D-glucose (K_i = 1.7 mM) [45] possibly because of the additional interactions of the 1,4-hydroquinone group with the protein residues.[25] Compared to **7**, the halogen substituted hydroquinones studied were found more potent inhibitors, with IC_{50} values (μM) comprised between 169.9 ± 10 (**3**) and 39.8 ± 0.3 (**5**).

Comparing compounds **16** and **3** reveals that the inhibitory potency does not change significantly by the replacement of the bromide group by a chloride. However, replacing the hydroxyl with a methoxy group and having a chloride on C-11of the aromatic ring (compound **5**), has a profound effect on potency, lowering the IC_{50} to 39.8 ± 0.3 μM (Table 1). An IC_{50} of 140 μM was measured for a mixture of compounds **3** (60%) and **4** (40%). From the IC_{50} value of pure **3** (169.9 μM) and using the compound composition in the mixture the IC_{50} of **4** was estimated to 95 μM. With respect to the lead compound **7** it seems that the addition of a chloride or a bromide atom to the aromatic ring has improved the potency of the inhibitors since all four compounds presented in this study have IC_{50} values 5–25 times lower than that of **7** for GPb (Fig. 2). Furthermore, bromine is more favorable than chlorine at C-10 (Table 1) while chlorine has a positive influence in potency at the C-11 (Table 1) position.

3.3. Structural studies

In order to elucidate the structural basis of inhibition we have determined the crystal structure of GPb in complex with each of the compounds **3, 5, 16**, and with the mixture of **3** and **4**. A summary of the data processing and refinement statistics for the inhibitor complex structures is given in Table 2. The $2F_o–F_c$ and $F_o–F_c$ electron density maps clearly defined the position of each atom of the inhibitors and specifically showed that all the studied compounds were bound at the catalytic site of GPb (Fig. 3).

Table 1
Inhibitory efficiency of the hydroquinone derivatives and the atom numbering scheme used in crystal structures

Compounds	Chemical structure	IC_{50} (μM)
7	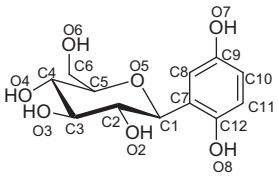	977[a]
16	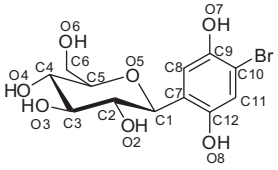	136.4 ± 4.9
3	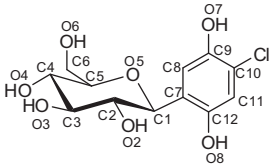	169.9 ± 10.0
Mixture of **3** and **4**	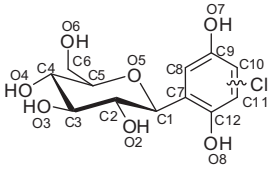	140.0 ± 10.0
4	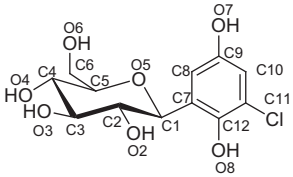	95[b]
5	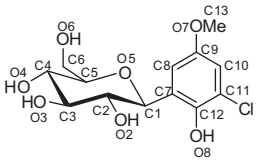	39.8 ± 0.3

[a] Value calculated from the K_i reported in. [25]
[b] Value calculated using the IC_{50} value of the mixture of **3** and **4**, the IC_{50} of pure **3** and a ratio of **3**:**4** in the mixture of 0.6:0.4.

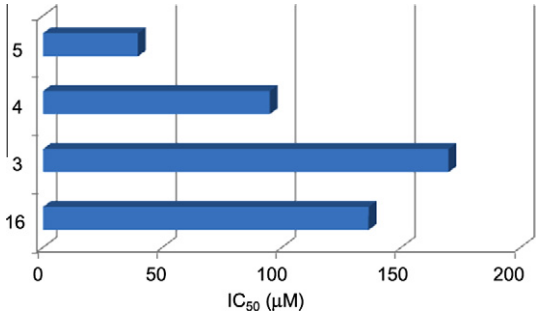

Figure 2. A schematic representation of the IC_{50} values of the four inhibitors studied.

Additional electron density was found in the GPb complex with the mixture of compounds **3** and **4** at a site distinct from the five known GPb binding sites (Fig. 4).

The superimposition of the structures of native GPb and the GPb–inhibitor complexes over well defined residues (18–249, 262–312, 326–829) gave rmsd values of 0.1 Å (mixture of **3** and **4**), 0.16 Å (**5**), 0.09 Å (**16**) and 0.1 Å (**3**) (Cα positions) indicating that the inhibitors were accommodated at the catalytic site without any major conformational change of the protein structure. The mode of binding and the hydrogen bonding network of interactions of the glucopyranose moiety are analogous to those observed for the glucopyranose moiety of the lead compound **7**[25] and other glucopyranose derivatives.[8–10,23] Thus, the hydroxyl groups of glucopyranose engage in hydrogen bond interactions with side chain atoms of Asn284, His377, Asn484, Tyr573 and Glu672, and with main chain atoms of Ala673, Ser674 and Gly675. Furthermore, three conserved water molecules mediate hydrogen bond interactions between the glucopyranose moiety of each ligand and main chain atoms of His377, Thr671, Ala673, Asp283 and Lys574, and the main and side chain atoms of Thr676 and the phosphate group of the co-factor PLP (Fig. 5).

Upon binding of the lead compound **7** to GPb the hydroquinone group is accommodated at the β-pocket of the catalytic site. There O8 makes direct polar interactions with Leu136N and Asp283 OD1, and water-mediated hydrogen bond interactions with Gly134N, Gly135N, Glu88 OE2, Asp283 OD1 and Asp283 OD2. Atom O7 also forms a hydrogen bond with Asp339 OD1 of the β-pocket.[25] In addition it participates in an extended network of van der Waals interactions with residues of the 280s loop.[25]

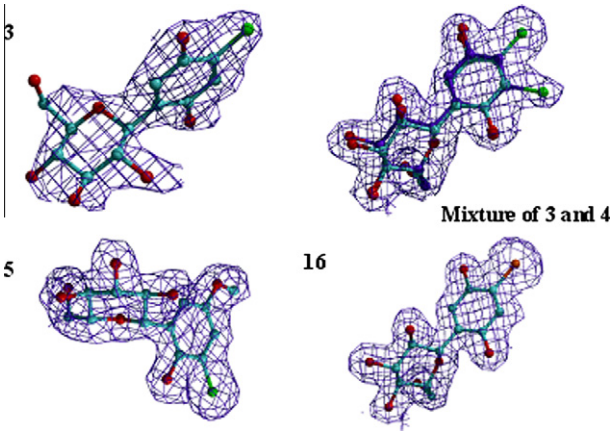

Figure 3. $2F_o$-F_c electron density maps of hydroquinone compounds bound at the catalytic site. The maps are contoured at 1σ level before the inclusion of the ligand molecule in the refinement process.

3.3.1. The binding of 2,5-dihydroxy-4-(β-D-glucopyranosyl)-bromo-benzene (16) and 2,5-dihydroxy-4-(β-D-glucopyranosyl)-chlorobenzene (3)

Upon binding to the catalytic site of GPb compound **16** forms 12 hydrogen bonds and 84 van der Waals interactions, while compound **3** forms 16 hydrogen bonds and 84 van der Waals interactions with protein residues (Table 2). The hydrogen bond pattern of the glycopyranose ring is the same for both compounds (Table 1), and compound **3** forms two additional hydrogen bonds; atom

Table 2
Summary of the diffraction data processing, refinement and protein ligand interactions statistics for GPb–inhibitor complexes

GPb complex	**16**	**3**	Mixture of **3** and **4**	**5**
Data collection and processing statistics				
Resolution (Å)	30.0–1.97	30.0–2.00	30.0–2.05	30.0–2.00
No. of observations	368,477	634,277	380,693	460,082
No. of unique reflections	64,845 (3109)	65,452 (3213)	60,600 (2641)	63,987 (3140)
R_{symm}[a]	0.065 (0.298)	0.040 (0.398)	0.061 (0.339)	0.050 (0.295)
Completeness (%)	93.9 (90.9)	98.7 (99.0)	86.8 (97.8)	98.0 (97.3)
Outermost shell (Å)	2.00–1.97	2.03–2.00	2.09–2.05	2.03–2.00
$\langle I/\sigma(I)\rangle$	11.3 (4.2)	21.2 (5.2)	14.8 (3.9)	16.1 (4.7)
Redundancy	3.7 (3.8)	5.4 (5.4)	3.9 (3.1)	4.0 (3.7)
B-values (Å^2)	26.5	31.1	29.8	22.3
Refinement statistics				
R_{cryst}[b]	0.19 (0.21)	0.19 (0.21)	0.19 (0.22)	0.19 (0.21)
R_{free}[c]	0.23 (0.26)	0.24 (0.27)	0.25 (0.29)	0.22 (0.249)
No. of solvent molecules	335	265	250	326
rms deviation from ideality				
In bond lengths (Å)	0.007	0.007	0.007	0.007
In bond angles (°)	1.022	1.028	1.039	0.014
Average B factor (Å^2)				
Protein atoms	27.5	35.0	32.3	24.9
Ligand atoms	20.1	25.0	19.7 (1a), 20.3 (1b), 51.7 (novel site)	14.3
Solvent molecules	35.2	39.8	35.8	31.9
No. of hydrogen/halogen bond interactions				
Glucose ring	9	11	8[d]	10
Aromatic moiety	3	5	3[d]	2
Halogen atom	0	0	1[d]	1
No. of van der Waals interactions				
Glucose ring	47	45	42[d]	42
Aromatic moiety	34	34	31[d]	33
Halogen atom	3	5	5[d]	3

[a] $R_{symm} = \Sigma_h\Sigma_i|I(h) - I_i(h)/\Sigma_h\Sigma_i I_i(h)$ where $I_i(h)$ and $I(h)$ are the ith and the mean measurements of the intensity of reflection h.
[b] $R_{cryst} = \Sigma_h|F_o - F_c|/\Sigma_h F_o$, where F_o and F_c are the observed and calculated structure factors amplitudes of reflection h, respectively.
[c] R_{free} is equal to R_{cryst} for a randomly selected 5% subset of reflections not used in the refinement. Values in parentheses are for the outermost shell.
[d] Values are for compound **4**.

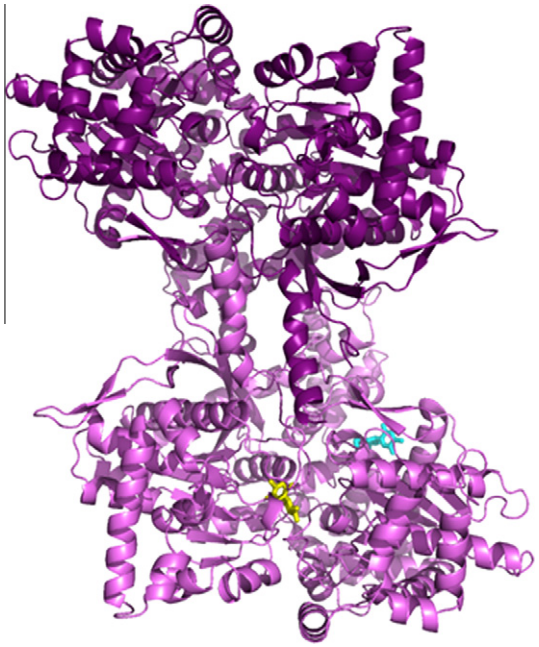

Figure 4. A schematic diagram of the GPb dimeric molecule viewed down the molecular dyad. One subunit is colored in dark purple and the other in light purple. The catalytic and the novel binding sites are marked by bound compound **3** (in yellow and cyan, respectively).

O2 with Asn284 OD1, and O3 with Ala673N. In both GPb-inhibitor complexes the hydroquinone group is accommodated at the β-pocket and O8 of the inhibitor is hydrogen bonded to residues of the glycine helix (134–150) Leu136N and Gly135N, Gly134N and Gly137N via Wat53 and Wat74. This atom is also hydrogen bonded to residues of the 280s loop (282–287) directly and via two water molecules (Fig. 5). Atom O7 takes part in hydrogen bond interactions with either one (compound **16**) or the two carboxyl oxygen atoms of the side chain of Asp339 (compound **3**). The bromide or the chloride group is not involved in any halogen bond interactions but both participate in 3 van der Waals interactions with His341 CE1, NE2 and Asn284N while the chloride group forms 2 additional van der Waals contacts with the side chain atoms of Asp339. Structural comparison of the GPb-**7,** GPb-**16** and GPb-**3** complexes revealed that all three inhibitors bind similarly to the active site and the existence of the halogen group triggered the displacement of one the conserved water molecules from the active site and the shift by 2.0 Å of another. Therefore the sevenfold and the 5.7-fold increase in the inhibitory potency of **16** and **3**, respectively, with respect to **7** may be attributed to the van der Waals interactions of the halogen group.

3.3.2. Binding of the mixture of structural isomers 2,5-dihydroxy-4-(β-D-glucopyranosyl)-chlorobenzene (3) and 2,5-dihydroxy-3-(β-D-glucopyranosyl)-chlorobenzene (4)

A solution of a mixture of the two structural isomers **3** and **4** (60% and 40%, respectively) was used for soaking GPb native crystals to obtain the enzyme–inhibitor complex. Thus, in the crystal structure both compounds **3** and **4** were found bound at the catalytic site of GPb with occupancies of 0.6 and 0.4, respectively, in a similar structural mode. Compound **3** is bound in an identical manner with the one found in the GPb-**3** complex described above. Upon binding to the catalytic site of GPb, compound **4** forms 11 hydrogen bonds and 78 van der Waals interactions (Table 2, Fig. 5). A structural comparison with the lead compound **7** reveals that all three inhibitors bind similarly within the active site of GPb (Fig. 6). The hydroquinone groups are accommodated at the β-pocket of the catalytic site and stabilize the closed conformation of the 280s loop. Thus, the hydroxyl group O7 makes direct polar interactions with Asp283 OD1 while O8 is involved in hydrogen bond interactions with Leu136N and Asp283 OD1, and water-mediated interactions with Glu88 OE2, Gly134N, Gly135N, Gly137N and Asp283 OD1 and OD2 (Fig. 5). The chloride at the C-11 position is involved in a direct halogen bond with OD1 of Asp283 and two water-mediated interactions with the main chain nitrogen of Gly134 and OE2 of Glu88 (Fig. 5). These interactions are possibly the main reason for the sevenfold increase in the inhibitory potency of the mixture of compounds **4** and **3** with respect to that of compound **7**. This is supported by the fact that compound **3** alone displays an IC_{50} of 169.9 μM (5.8 times smaller compared to that of **7**). Furthermore, the direct halogen interactions of the chloride group at position C-11 (compound **4**) with GPb residues along with its water-mediated interactions which do not exist when chloride is in C-10 position (compound **3**) seem to form the structural basis of the increased potency of compound **4** with respect to that of **3**.

In the GPb complex structure with the mixture of **3** and **4** compound **3** was also found bound to a new site of GPb. This novel binding site is located ~27 Å from the catalytic site, ~38 Å from the allosteric site and ~45 Å from the new allosteric site (Fig. 4). This binding pocket is formed by residues 122–124 (of the α5-helix residues 118–124), residues 124–129 (of the β3 strand-residues 129–131), residues 494–508 (of the α16 helix-residues 496–508), residues 527–553 (of the α17 helix-residues 527–553) and residues 649–657 (of the α20 helix-residues 649–657). The inhibitor is surrounded by a hydrophobic environment formed by the aromatic amino acids Tyr548 and Phe545. It is also surrounded by Lys545 and Lys544. Lysine contains four methylene groups capped by an ammonium ion at neutral pH. Although sometimes lysine is considered as a hydrophylic amino acid, the apolar methylene groups of the residue often participate in favorable hydrophobic interactions within folded peptides and proteins. In addition, when found in a hydrophobic environment, lysine stabilizes this environment by forming salt bridges. Therefore, it is likely to assume that these two lysines surrounding the binding pocket possibly play a role in stabilizing the hydrophobic environment surrounding the inhibitor. It is noteworthy that O2, O3 and O4 of glucose are exposed to the solvent. O2 forms a hydrogen bond with Lys544, while O4 forms a hydrogen bond with Leu494 and Gln96 (Fig. 7) and O7 forms a hydrogen bond with Lys655 via a water molecule. Chloride forms a halogen bond to the main chain carbonyl oxygen of Lys544. Overall, upon binding to the enzyme, the inhibitor forms 6 hydrogen bonds and 61 van der Waals interactions (Fig. 7). The number of hydrogen bonds is reduced as compared to the number observed for the catalytic site. Compounds **5** or **16** were not found bound at this site. It is interesting that compound **3** was found bound at this site only when GPb crystals were soaked with a mixture of compounds **3** and **4** and not when soaked with a solution of compound **3** alone. Presumably, this can be attributed to differences between the experimental conditions for forming these protein inhibitor complexes and those for forming the GPb-mixture of **3** and **4** or GPb-**3** complexes (if lower inhibitor concentration of the soaking solution and shorter soaking time were applied). However, experimental conditions were similar when soaking GPb native crystals with either a solution of a mixture of compounds **3** and **4** (100 mM, 21 h) or a solution of **3** (70 mM, 20 h). Therefore it is not clear whether this new site represents a genuine new binding site with a regulatory function or it is an artifact of the experiment conditions. However, it has to be noted that since from the mixture of compounds **3** and **4** only **3** binds to this site, the site displays some sort of specificity.

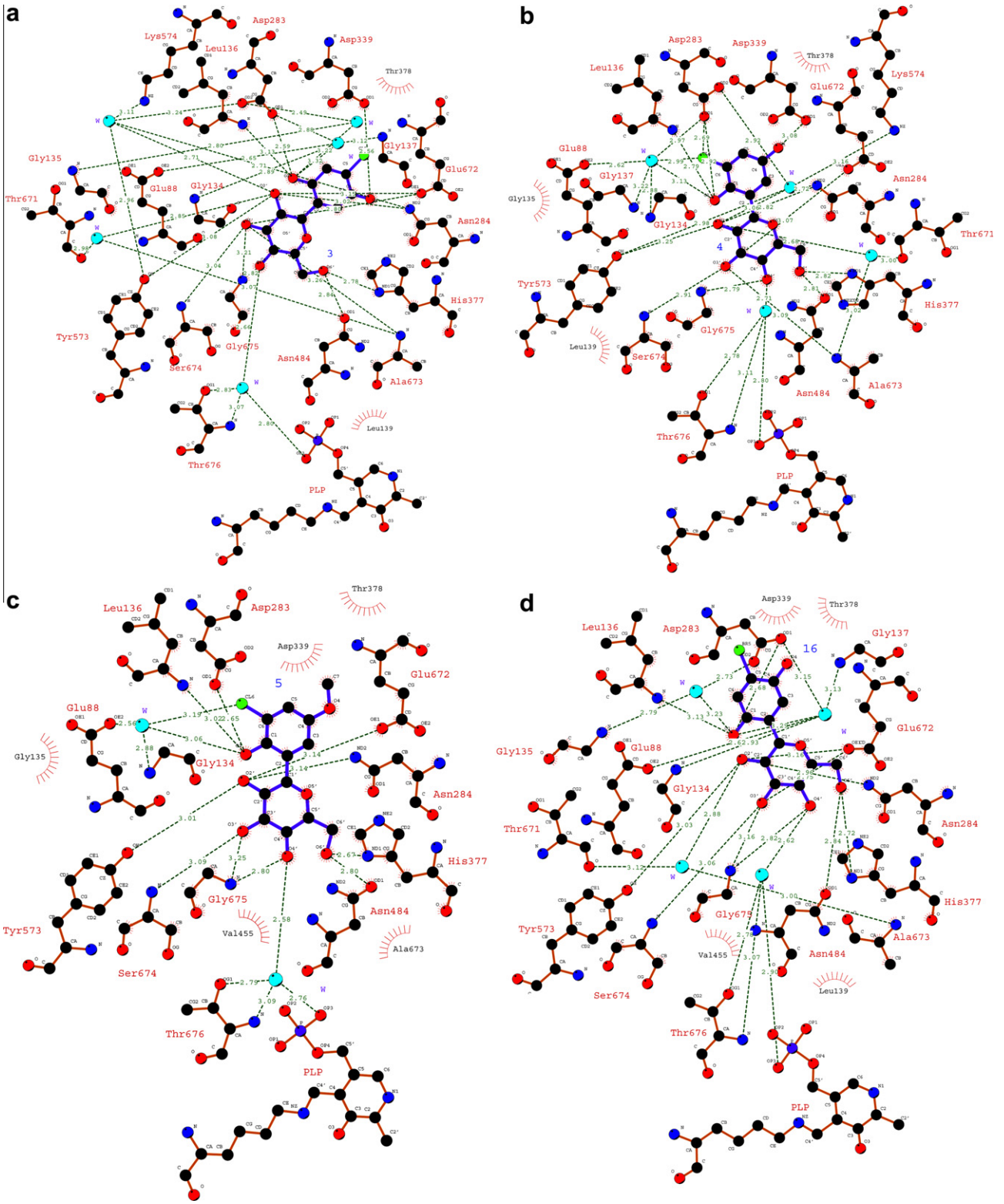

Figure 5. LIGPLOT[46] diagram of the network of interactions of **3** (a), **4** (b) **5** (c) and **16** (d) with GPb residues in the vicinity of the catalytic site. Hydrogen bonds are represented by green dashed lines and hydrophobic contacts by arcs with radiating spokes. Corresponding atoms, involved in hydrophobic contacts, are represented by black circles

3.3.3. Binding of 3-(β-D-glucopyranosyl)-2-hydroxy-5-methoxy-chlorobenzene (5)

Upon binding to the catalytic site of GPb the inhibitor **5** forms 12 hydrogen bonds (one more than **4**) and 79 van der Waals interactions with protein residues. It also participates in an extensive network of water-mediated interactions, stabilizing the 280s loop and hence the T state of the enzyme (Fig. 5). A structural comparison between the GPb-**7** and the GPb-**5** complexes revealed that the two inhibitors bind similarly to the enzyme's active site forming a similar hydrogen bond and van der Waals interactions

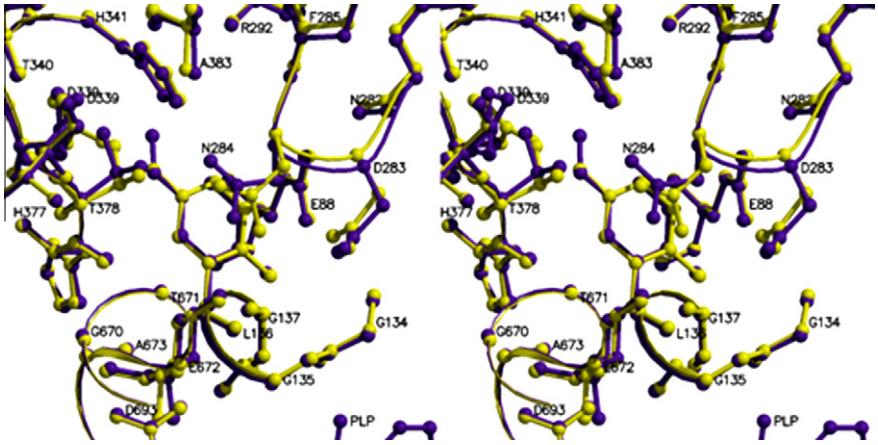

Figure 6. A structural comparison between inhibitors **5** (purple) and **7** (yellow) at the catalytic site of GPb in stereo.

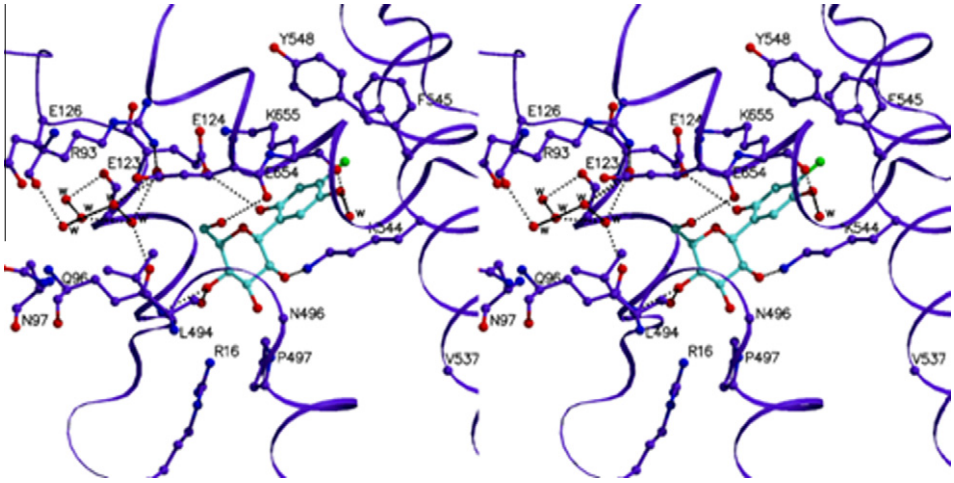

Figure 7. Stereo diagram showing the network of interactions formed between inhibitor **3** and residues at the novel binding site of GPb. Inhibitor molecules are shown in cyan and GPb residues in purple.

network with GPb residues. The chloride group of **5**, like that of **4**, is involved in a halogen interaction with Asp283 OD1 (albeit weak since the distance is 3.36 Å) and water-mediated halogen interactions with Leu136N and Gly137N. Comparative structural analysis of the GPb-**4** and the GPb-**5** complexes has shown that the two compounds bind similarly to the active site of the enzyme. However, the hydrogen bond interactions of hydroxyl O7 of compound **4** to Asp283 OD1 does not exist in the complex with compound **5** but it seems that the 8 additional van der Waals interactions of the methoxy group counteract this loss. Furthermore, these interactions are possibly responsible for the 2.4 times increase in the inhibitory potency of compound since **5** with respect to **4**.

4. Conclusions

In summary, the kinetic and structural studies of the binding of derivatives of C-glucosylhydroquinone showed that these compounds are potent competitive inhibitors of GPb with respect to Glc-1-P and bind at the catalytic site of the enzyme. One of the inhibitors was also found bound at a novel site of GPb. On binding to the enzyme, the inhibitors stabilize the less active T state of the enzyme through an extensive network of direct and water-mediated hydrogen and halogen bonds, as well as a network of van der Waals interaction with residues of the 280s loop (Asn283 and Asn284), the glycine helix (Gly134, and Gly137) and Glu88 and Asp339. These interactions serve to stabilize a conformation of the 280s loop that blocks access of the substrate glycogen to the catalytic site. Furthermore, the halogen interactions provide a rationale for the increased potency of these halogen derivatives glucosyl(hydro)quinones to inhibit GPb activity with respect to the lead compound, and should assist in the design of more effective compounds. Thus, it seems, that bromine substitution is more favorable than chlorine at C-10 position, chlorine has more favorable interactions at C-11 position, and a methoxy group at C-9 position is better than a hydroxyl group.

This study is part of an ongoing project to discover new GP inhibitors, as potential drugs against type 2 diabetes and although GP is a well documented enzyme, the findings presented here offer new possibilities for structure based drug design of type 2 diabetes, and proves that new pathways are yet to be exploited. Thus, this study shows that C-β-D-glucopyranosyl hydroquinones, in which the glucose moiety is linked by a highly stable C-glucosidic bond to a hydroquinone ring are well suited for regioselective modifications of the aglycon that modulate the binding to GP and inhibitory properties. More work in this series, possibly with the help of calculations and predictive methods should result in the design and synthesis of accessible, hydrolytically stable and more potent GPis, which will be subjected to further tests with cells and animals to better evaluate their potential as anti-hyperglycemic molecules.

Acknowledgments

This work was supported by the EU Marie Curie Early Stage Training (EST) contract no. MEST-CT-020575 and by the Commission of the European Communities—under the FP7 'SP4-Capacities Coordination and Support Action, Support Actions' EUROSTRUCT project (CSA-SA_FP7-REGPOT-2008-1 Grant Agreement N° 230146). This work was also supported by grants from European Community — Research Infrastructure Action under the FP6 'Structuring the European Research Area' Program (through the Integrated Infrastructure Initiative 'Integrating Activity on Synchrotron and Free Electron Laser Science') for work at the Synchrotron Radiation Source MAX-lab, Lund, Sweden, and EMBL Hamburg Outstation, Germany. Région Rhône-Alpes is warmly thanked for a stipend (Z.Y.Z.) and generous financial support allocated in the frame of the MIRA collaborative programme with Shanghai City (MIRA Recherche 2005). Other financial supports from CNRS (France), University Claude-Bernard Lyon 1 (for co-tutored PhD), ARCUS-Chine 2005 (joint support from Région Rhône-Alpes and French Ministry of Foreign Affairs), and the French Agence Nationale de Recherche (support of the ANR project GPdia N° ANR-08-BLAN-0305) are gratefully acknowledged.

Supplementary data

Supplementary data (inhibitor hydrogen bond and van der Waals interactions) associated with this article can be found, in the online version, at doi:10.1016/j.bmc.2011.07.024.

References

1. Green, A.; Hirsch, N. C.; Pramming, S. K. *Diabetes Metab. Res. Rev.* **2003**, *19*, 3.
2. Alberti, G.; Zimmet, P.; Shaw, J.; Bloomgarden, Z.; Kaufman, F.; Silink, M. *Diabetes Care* **2004**, *27*, 1798.
3. Bril, A.; Ktorza, A. *Curr. Opin. Pharmacol.* **2006**, *6*, 577.
4. Ross, S. A.; Gulve, E. A.; Wang, M. *Chem. Rev.* **2004**, *104*, 1255.
5. Das, S. K.; Chakrabarti, R. *Mini-Rev. Med. Chem.* **2005**, *5*, 1019.
6. Skyler, J. S. *J. Med. Chem.* **2004**, *47*, 4113.
7. Cori, C. F.; Cori, G. T. *Proc. Soc. Exp. Biol. Med.* **1936**, *34*, 702.
8. Oikonomakos, N. G. *Curr. Protein Pept. Sci.* **2002**, *3*, 561.
9. Oikonomakos, N. G.; Somsak, L. *Curr. Opin. Investig. Drugs* **2008**, *9*, 379.
10. Somsak, L.; Czifrak, K.; Toth, M.; Bokor, E.; Chrysina, E. D.; Alexacou, K. M.; Hayes, J. M.; Tiraidis, C.; Lazoura, E.; Leonidas, D. D.; Zographos, S. E.; Oikonomakos, N. G. *Curr. Med. Chem.* **2008**, *15*, 2933.
11. Treadway, J. L.; Mendys, P.; Hoover, D. J. *Expert Opin. Investig. Drugs* **2001**, *10*, 439.
12. Baker, D. J.; Timmons, J. A.; Greenhaff, P. L. *Diabetes* **2005**, *54*, 2453.
13. Hayes, J. M.; Leonidas, D. D. *Mini-Rev. Med. Chem.* **2010**, *10*, 1156.
14. Chrysina, E. D. *Mini-Rev. Med. Chem.* **2010**, *10*, 1093.
15. Praly, J.-P.; Vidal, S. *Mini-Rev. Med. Chem.* **2010**, *10*, 1102.
16. Agius, L. *Mini-Rev. Med. Chem.* **2010**, *10*, 1175.
17. Benltifa, M.; Vidal, S.; Gueyrard, D.; Goekjian, P. G.; Msaddek, M.; Praly, J.-P. *Tetrahedron Lett.* **2006**, *47*, 6143.
18. Benltifa, M.; Hayes, J. M.; Vidal, S.; Gueyrard, D.; Goekjian, P. G.; Praly, J.-P.; Kizilis, G.; Tiraidis, C.; Alexacou, K. M.; Chrysina, E. D.; Zographos, S. E.; Leonidas, D. D.; Archontis, G.; Oikonomakos, N. G. *Bioorg. Med. Chem.* **2009**, *17*, 7368.
19. Somsak, L.; Nagy, V.; Vidal, S.; Czifrak, K.; Berzsenyi, E.; Praly, J.-P. *Bioorg. Med. Chem. Lett.* **2008**, *18*, 5680.
20. Nagy, V.; Benltifa, M.; Vidal, S.; Berzsenyi, E.; Teilhet, C.; Czifrak, K.; Batta, G.; Docsa, T.; Gergely, P.; Somsak, L.; Praly, J.-P. *Bioorg. Med. Chem.* **2009**, *17*, 5696.
21. Benltifa, M.; Vidal, S.; Fenet, B.; Msaddek, M.; Goekjian, P. G.; Praly, J.-P.; Brunyanszki, A.; Docsa, T.; Gergely, P. *Eur. J. Org. Chem.* **2006**, 4242.
22. Toth, M.; Kun, S.; Bokor, E.; Benltifa, M.; Tallec, G.; Vidal, S.; Docsa, T.; Gergely, P.; Somsak, L.; Praly, J.-P. *Bioorg. Med. Chem.* **2009**, *17*, 4773.
23. Tsirkone, V. G.; Tsoukala, E.; Lamprakis, C.; Manta, S.; Hayes, J. M.; Skamnaki, V. T.; Drakou, C.; Zographos, S. E.; Komiotis, D.; Leonidas, D. D. *Bioorg. Med. Chem.* **2010**, *18*, 3413.
24. Praly, J.-P.; He, L.; Qin, B. B.; Tanoh, M.; Chen, G. R. *Tetrahedron Lett.* **2005**, *46*, 7081.
25. He, L.; Zhang, Y. Z.; Tanoh, M.; Chen, G. R.; Praly, J.-P.; Chrysina, E. D.; Tiraidis, C.; Kosmopoulou, M.; Leonidas, D. D.; Oikonomakos, N. G. *Eur. J. Org. Chem.* **2007**, 596.
26. He, L.; Galland, S.; Dufour, C.; Chen, G. R.; Dangles, O.; Fenet, B.; Praly, J.-P. *Eur. J. Org. Chem.* **2008**, 1869.
27. Zhang, Y. Z.; Aouadi, K.; Chen, G.-R.; Praly, J.-P. *Synthesis* **2007**, 3473.
28. Kuribayashi, T.; Mizuno, Y.; Gohya, S.; Satoh, S. *J. Carbohydr. Chem.* **1999**, *18*, 371.
29. Melpidou, A. E.; Oikonomakos, N. G. *FEBS Lett.* **1983**, *154*, 105.
30. Saheki, S.; Takeda, A.; Shimazu, T. *Anal. Biochem.* **1985**, *148*, 277.
31. Oikonomakos, N. G.; Melpidou, A. E.; Johnson, L. N. *Biochim. Biophys. Acta* **1985**, *832*, 248.
32. Otwinowski, Z.; Minor, W. In *Methods Enzymol*; Carter, C. W. J., Sweet, R. M., Eds.; Academic Press: New York, 1997; Vol. 276, p 307.
33. Murshudov, G. N.; Vagin, A. A.; Dodson, E. J. *Acta Crystallogr., Sect. D* **1997**, *53*, 240.
34. Emsley, P.; Cowtan, K. *Acta Crystallogr., Sect. D* **2004**, *60*, 2126.
35. Laskowski, R. A.; MacArthur, M. W.; Moss, D. S.; Thornton, J. M. *J. Appl. Crystallogr.* **1993**, *26*, 283.
36. CCP4 *Acta Crystallogr., Sect. D* **1994**, *50*, 760.
37. Kraulis, P. J. *J. Appl. Crystallogr.* **1991**, *24*, 946.
38. DeLano, W. L.; Sa Carlos: CA, USA, 2002.
39. Merritt, E. A.; Bacon, D. J. *Macromol. Crystallogr.* **1997**, *B277*, 505.
40. Schnabelrauch, M.; Vasella, A.; Withers, S. G. *Helv. Chim. Acta* **1994**, *77*, 778.
41. March, J. *Advanced Organic Chemistry: Reactions, Mechanisms, and Structure*; John Wiley & Sons, 1992.
42. Carreno, M. C.; Ruano, J. L. G.; Sanz, G.; Toledo, M. A.; Urbano, A. *J. Org. Chem.* **1995**, *60*, 5328.
43. Tanemura, K.; Suzuki, T.; Nishida, Y.; Satsumabayashi, K.; Horaguchi, T. *Chem. Lett.* **2003**, *32*, 932.
44. Miller, L. L.; Stewart, R. F. *J. Org. Chem.* **1978**, *43*, 3078.
45. Martin, J. L.; Veluraja, K.; Ross, K.; Johnson, L. N.; Fleet, G. W. J.; Ramsden, N. G.; Bruce, I.; Orchard, M. G.; Oikonomakos, N. G.; Papageorgiou, A. C.; Leonidas, D. D.; Tsitoura, H. S. *Biochemistry (USA)* **1991**, *30*, 10101.
46. Wallace, A. C.; Laskowski, R. A.; Thornton, J. M. *Protein Eng.* **1995**, *8*, 127.